Self-assembly of nanoscopic coordination cages of D_{3h} symmetry

Christopher J. Kuehl*, Yury K. Kryschenko*, Ukkirampandian Radhakrishnan*, S. Russell Seidel*, Songping D. Huang†, and Peter J. Stang*‡

*Department of Chemistry, University of Utah, Salt Lake City, UT 84112; and †Department of Chemistry, Kent State University, Kent, OH 44242

Contributed by Peter J. Stang, October 11, 2001

A family of nanoscale-sized supramolecular cage compounds with a trigonal prismatic framework was prepared by means of spontaneous self-assembly from the combination of a predesigned molecular "clip" with tritopic pyridyl subunits. As confirmed by x-ray crystallography, the smallest structure of the reported series is ≈1 × 2 nm and possesses a nitrate anion incarcerated inside its molecular cavity. The largest structure has dimensions of ≈ 1 × 4 nm.

The formation of discrete supramolecular entities driven and held together by metal coordination is an intense new area of investigation at the forefront of supramolecular chemistry (1–10). Because self-assembly is guided by the chemical information encoded into the molecular subunits, diverse structures with predetermined shape, size, and functionality can readily be designed. Indeed, a wide variety of aesthetic structures have been realized, such as molecular grids, helicates, rings, catenanes, tetrahedra, cubes, cuboctahedra, etc. Once assembled, many of the hollow structures have been shown to be capable of encapsulating molecules through electrostatic and/or dispersion forces. Often times, ions will template the formation of an assembly (11–21). When considering that metal-containing assemblies often possess magnetic, photophysical, and/or redox properties not accessible from purely organic systems, studies in basic host–guest chemistry hold new promise for technologies in molecular sensing (22–28), separations, and catalysis (29, 30).

Because lower-symmetry hosts can ultimately be expected to show enhanced guest selectivity, especially toward planar aromatic guests, prismatic cages represent a natural progression in the development of this area. Although M_3L_2-type cages are relatively simple three-dimensional constructs, they remain uncommon. Of those that have been reported (31–40), most usually either require the use of templates to assemble in solution, or assemble only in the solid state. Part of the reason for this limitation is possibly the fact that, in most cases, flexible ligands were used. By contrast, structures derived from *rigid* tritopic linkers with *cis*-metal ions are either: (*i*) tetrahedral M_6L_4 cages (41) where L is a planar ligand, or (*ii*) double-square M_6L_4 cages (42) where L is a 109° linker ligand. Construction of the M_3L_2, D_{3h} species is complicated by the fact that rigid tritopic linkers with ideal mutual angles of 60° are not easily accessible. A noteworthy trigonal bipyramidal structure (35), made from Pd(II) ions and a calix[3]arene subunit, was shown to be able to reversibly bind a molecule of C_{60}.

By exploiting incommensurate symmetry requirements for differing metallic subunits, an alternative approach to structures of this general topology was recently reported. Raymond and Wong (43–45) successfully prepared a series of $M_2M'_3L_6$ supramolecular clusters where a multifunctionalized ligand (L) was cleverly designed to selectively interact with two types of metal ions (one hard and one soft).

Double oxidative addition to rigid aromatic ligands offers a unique way to direct the open coordination sites of metals (46), because nearly any desired angle can be fashioned provided the corresponding aryl halide is accessible. Presented here is a ligand-directed approach to molecular prisms, thus providing a versatile method for the construction of supramolecular structures of variable size and functionality, in high yield, and without the use of templates. Specifically, the modular self-assembly of a new family of metalla-bicyclic structures (**3a–3c**), directed by a molecular "clip" (**1**) as a preconstructed shape-defining unit, is described. The structure and properties of these nanoscopic, macrocyclic species have been studied by electrospray ionization (ESI)-mass spectrometry, multinuclear NMR, and x-ray crystallography.

Experimental Section

General Methods. Building unit **2a** (47) was synthesized by a published method and **2b** and **2c** were prepared in an analogous manner. NMR spectra were recorded on a Varian XL-300 or a Unity 300 spectrometer. Deuterated solvents were used as received. Proton chemical shifts are reported relative to residual protons of the deuterated acetone (δ 2.05). ^{31}P $\{^1H\}$ chemical shifts (δ) are reported relative to an unlocked, external sample of H_3PO_4 (0.0 ppm). Elemental analyses were performed by Atlantic Microlab, Norcross, GA.

General Procedure for the Preparation of Compounds 3a–3c. In a 2-dram (8 g) vial equipped with a magnetic stir bar were placed solid 1,8-bis(*trans*-$Pt(PEt_3)_2(NO_3)$)anthracene (20.0 mg, 0.0172 mmol) with a 0.67 molar ratio of the appropriate tritopic bridging ligand. Next, 1 ml of an acetone-d_6/D_2O mixture was added to the vial (1:1 for **3a**, 1:2 for **3b** and **3c**), which was then sealed with Teflon tape and heated in an oil bath at 50–55°C, with stirring. After the specified length of time (3–5 h for **3a**, 20–24 h for **3b** and **3c**), the initial pale yellow suspension gradually became homogeneous. The solution was then transferred to an NMR tube for analysis. The product was precipitated with KPF_6, collected on a frit, washed with excess water, and dried *in vacuo*.

Bicyclo[Tris[1,8-bis(*trans*-$Pt(PEt_3)_2(NO_3)$)anthracene)]bis[Tris(4-pyridyl)methanol]] (3a). ^1H NMR (acetone-d_6/D_2O, 300 MHz): δ 9.18 (d, 6H, $^3J_{HH}$ = 6.3 Hz, $H_{\alpha\text{-Py}}$), 8.98 (m, 9H, $H_{\alpha\text{-Py}}$, H_9), 8.37 (s, 3H, H_{10}), 8.31 (d, 6H, $^3J_{HH}$ = 6.0 Hz, $H_{\beta\text{-Py}}$), 7.75 (m, 12H, $H_{\beta\text{-Py}}$, $H_{4,5}$), 7.69 (d, 6H, $^3J_{HH}$ = 7.8 Hz, $H_{2,7}$), 7.14 (m, 6H, $H_{3,6}$), 1.40 (m, 72H, PCH_2CH_3), 0.89 (m, 108H, PCH_2CH_3). $^{31}P\{^1H\}$ NMR (acetone-d_6/D_2O, 121.4 MHz): δ 9.5 (s, $^1J_{PPt}$ = 2,652 Hz). ESI-MS: 2,069 [calculated for $(M - 2PF_6)^{2+}$: 2,069], 1,331 [calculated for $(M - 3PF_6)^{3+}$: 1,331]. Analysis calculated for $C_{196}H_{230}F_{30}N_7O_5P_{17}Pt_6$: C, 39.58; H, 5.23; N, 2.21. Found: C, 39.64; H, 5.24; N, 2.21.

Bicyclo[Tris[1,8-bis(*trans*-$Pt(PEt_3)_2(NO_3)$)anthracene]bis[1,3,5-Tris(4-ethynylpyridyl)adamantane]] (3b). ^1H NMR (acetone-d_6/D_2O, 300 MHz): δ 9.17 (s, 3H, H_9), 8.95 (d, 6H, $^3J_{HH}$ = 5.7 Hz, $H_{\alpha\text{-Py}}$), 8.76

Abbreviation: ESI, electrospray ionization.

Data deposition: The atomic coordinates have been deposited in the Cambridge Structural Database, Cambridge Crystallographic Data Centre, Cambridge CB2 1EZ, United Kingdom (CSD reference nos. 172584 and 172585).

‡To whom reprint requests should be addressed at: Chemistry Department, University of Utah, 315 South 1400 East, Room 2020, Salt Lake City, UT 84112. E-mail: stang@chem.utah.edu.

 www.pnas.org/cgi/doi/10.1073/pnas.012540799

Table 1. Crystal data and structure refinement results for 3a and 3c

Empirical formula	$C_{146}H_{230}F_{36}N_6O_2P_{18}Pt_6$ **(3a)**	$C_{194}H_{258}F_{36}N_6P_{18}Pt_6$ **(3c)**
Formula weight	4,513.36	5,086.06
Color/shape	Yellow/trigonal prism	
Crystal system	Triclinic	Rhombohedral
Space group	$P\bar{1}$ (#2)	$R\bar{3}c$ (#167)
Unit cell dimensions	a = 20.6055(5) Å	a = 30.6988(2) Å
	b = 20.8610(5) Å	b = 30.6988(2) Å
	c = 29.2406(5) Å	c = 52.3624(8) Å
	α = 79.88(1)°	α = 90.00°
	β = 69.55(1)°	β = 90.00°
	γ = 61.39(1)°	γ = 120.00°
Volume	10,337.9(4) Å^3	42,735.9(8)
Z	2	6
Density (calculated)	1.450 mg/m^3	1.186 mg/m^3
Absorption coefficient	4.257 mm^{-1}	3.096 mm^{-1}
F(000)	4,452	15,156
Crystal size	0.31 × 0.19 × 0.17 mm	0.24 × 0.17 × 0.15
θ Range for data collection	1.49 to 28.40	1.72 to 28.21
Reflections collected	123,286	11,538
Independent/observed reflections	48,757 (R_{int} = 0.088)/23700 ([I > 2σ(I)])	88,416 (R_{int} = 0.1265)/4256 ([I > 2σ(I)])
Absorption correction	Semiempirical from simulated Ψ-scans	Semiempirical from simulated Ψ-scans
Range of relative transmission factors	1.00, 0.841	1.00, 0.883
Final R indices [I > 2σ(I)]	R = 0.0634, Rw = 0.1688	R = 0.1492, Rw = 0.3827
Goodness-of-fit on F	0.965	1.300
Weighting scheme	$1/[\sigma^2(F_o^2) + (0.1064P)^2 + 0.0000P]$ where $P = (F_o^2 + 2F_c^2)/3w$	$1/[\sigma^2(F_o^2) + (0.2000P)^2 + 0.0000P]$, where $P = (F_o^2 + 2F_c^2)/3w$
Largest difference peak and hole	3.47 and −2.33 eÅ^{-3}	3.77 and −1.08 eÅ^{-3}

(d, 6H, $^3J_{HH}$ = 5.7 Hz, $H_{\alpha\text{-Py}}$), 8.32 (s, 3H, H_{10}), 7.85 (m, 12H, $H_{\beta\text{-Py}}$), 7.66 (m, 12H, $H_{2,4,5,7}$), 7.13 (m, 6H, $H_{3,6}$), 1.37 (m, 72H, PCH_2CH_3), 0.82 (m, 108H, PCH_2CH_3). $^{31}P\{^1H\}$ NMR (acetone-d_6/D_2O, 121.4 MHz): δ 8.9 (s, $^1J_{PPt}$ = 2,656 Hz). ESI-MS: 2287 [calculated for $(M - 2PF_6)^{2+}$: 2,287], 1,476 [calculated for $(M - 3PF_6)^{3+}$: 1,476), 1,071 [calculated for $(M - 4PF_6)^{4+}$: 1,071). Analysis calculated for $C_{204}H_{272}F_{36}N_6P_{18}Pt_6$: C, 46.94; H, 5.25; N, 1.61. Found: C, 47.07; H, 5.27; N, 1.71.

Bicyclo[Tris[1,8-bis(*trans*-Pt(PEt$_3$)$_2$(NO$_3$))anthracene]bis[1,1,1-Tris(4-phenyl(4′-ethynylpyridyl)ethane]] (3c). ^1H NMR (acetone-d_6/D_2O, 300 MHz): δ 9.33 (s, 3H, H_9), 9.06 (d, 6H, $^3J_{HH}$ = 5.4 Hz, $H_{\alpha\text{-Py}}$), 8.91 (d, 6H, $^3J_{HH}$ = 5.7 Hz, $H_{\alpha\text{-Py}}$), 8.40 (s, 3H, H_{10}), 8.03 (m, 12H, $H_{\beta\text{-Py}}$), 7.73 (d, 6H, $^3J_{HH}$ = 8.7 Hz, $H_{4,5}$), 7.71 (d, 6H, $^3J_{HH}$ = 6.0 Hz, $H_{2,7}$), 7.62 (d, 12H, $^3J_{HH}$ = 8.4 Hz, $H_{3,5\text{-phenylene}}$), 7.24 (d, 12H, $^3J_{HH}$ = 8.7 Hz, $H_{2,6\text{-phenylene}}$), 7.17 (m, 6H, $H_{3,6}$), 1.46 (m, 72H, PCH_2CH_3), 0.87 (m, 108H, PCH_2CH_3). $^{31}P\{^1H\}$ NMR

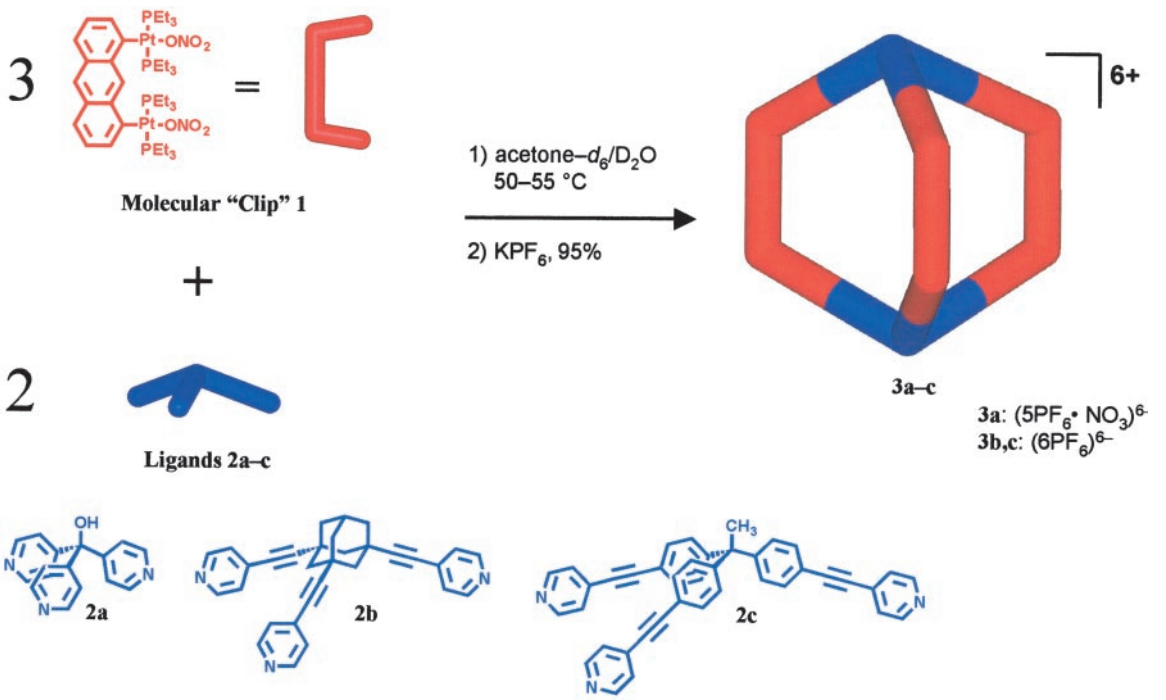

Scheme 1. Self-assembly of coordination cages **3a–3c**.

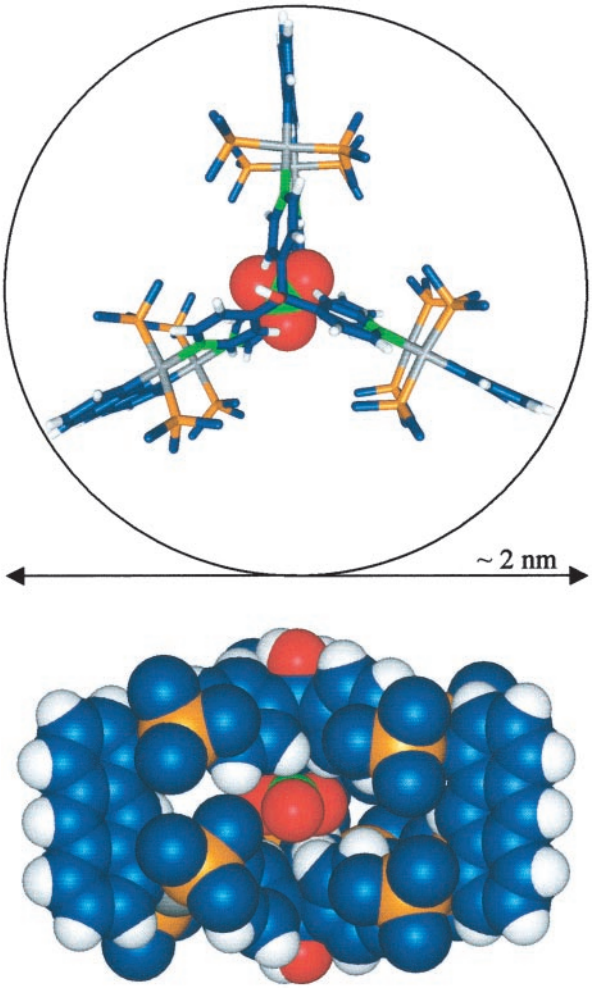

Fig. 1. Two perspectives of the x-ray structure of **3a**. (*Upper*) The framework is shown as a stick model, and the encapsulated nitrate is represented with a space-filling model. All other counterions and the methyl groups from the triethylphosphines are omitted for clarity. (*Lower*) Space-filling model viewed down the C_2 axis. Colors: C, blue; H, white; N, green; O, red; P, orange; Pt, gray.

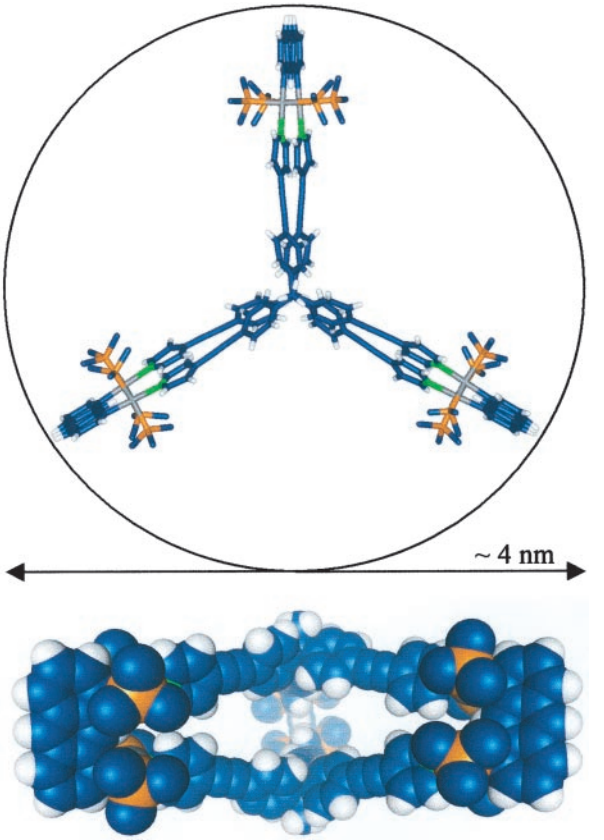

Fig. 2. Two perspectives of the x-ray structure of **3c**. (*Upper*) Stick model as viewed down the C_3 axis. Counterions and the methyl groups from the triethylphosphines are omitted for clarity. (*Lower*) Space-filling model viewed down the C_2 axis. Colors: C, blue; H, white; N, green; P, orange; Pt, gray.

(acetone-d_6/D_2O, 121.4 MHz): δ 8.8 (s, $^1J_{PPt}$ = 2,641 Hz). ESI-MS: 2409 [calculated for $(M - 2PF_6)^{2+}$: 2,409], 1,557 [calculated for $(M - 3PF_6)^{3+}$: 1557), 1,132 [calculated for $(M - 4PF_6)^{4+}$: 1,132]. Analysis calculated for $C_{196}H_{258}F_{36}N_6P_{18}Pt_6$: C, 46.07; H, 5.09; N, 1.64. Found: C, 45.26; H, 5.03; N, 1.74.

X-Ray Data Collection, Structure Solution, and Refinement. A single crystal of either **3a** or **3c** was selected from the reaction product and mounted on a thin glass fiber by using silicone grease. The data were collected at −100°C, using a narrow frame method with scan widths of 0.3° in ω and exposure times of 20 s. A hemisphere of intensity data were collected in 1,081 frames with the crystal-to-detector distance of 50.4 mm, which corresponds to a maximum 2θ value of 54.1°. Frames were integrated with the Bruker SAINT program (Billerica, MA). A semiempirical absorption correction based on simulated ψ-scans was applied to the data set. Both structures were solved by a combination of direct methods and difference Fourier methods, and refined with full-matrix least squares techniques. Details of the data collection, structure solution, and refinement are given in Table 1. Tables of the atomic coordinates, thermal displacement parameters, and selected bond distances and angles complete with ORTEP representations of **3a** and **3c** are provided in the supporting information, which is published on the PNAS web site, www.pnas.org.

Results and Discussion

The preparation of several discrete nanoscopic cage complexes can be achieved with simplicity and, given the proper conditions, in essentially quantitative yield. The assembly of these cages is most easily monitored by their ^1H and $^{31}P\{^1H\}$ NMR spectra. For example, on gentle heating, a suspension of a 3:2 stoichiometric combination of **1** and **2a** in a 1:1 (vol:vol) acetone-d_6/D_2O mixture (Scheme 1) gradually dissolves (3 h) to give a bright yellow homogeneous solution of the smallest molecular cage assembly described in this paper, structural motif **3a**. $^{31}P\{^1H\}$ NMR (121.4 MHz) analysis of the reaction solution is consistent with the formation of a highly symmetrical species by the appearance of a sharp singlet with concomitant ^{195}Pt satellites, shifted 5.0 ppm upfield ($-\Delta\delta$) relative to **1** ($\Delta^1J_{PPt} = -203$ ppm). Likewise, reaction of component **1** with tritopic bridging ligands **2b** and **2c** yielded the analogous molecular cages **3b** and **3c**, respectively, of differing dimensions and topology (Scheme 1).

Examination of the ^1H NMR (300 MHz) spectra of cages **3a**–**3c** was also indicative of highly symmetrical structures and displayed significant spectroscopic differences from their monomeric subunits. Particularly diagnostic were the significant downfield shifts of the pyridyl signals ($\Delta\delta \approx 0.5$ ppm), associated with the loss in electron density on coordination by the nitrogen lone pair to the platinum metal center. In accordance with previously reported molecular rectangles (48, 49), the inner and outer pyridyl protons were found to be inequivalent because of restricted rotation around the platinum–pyridine bond (50–54).

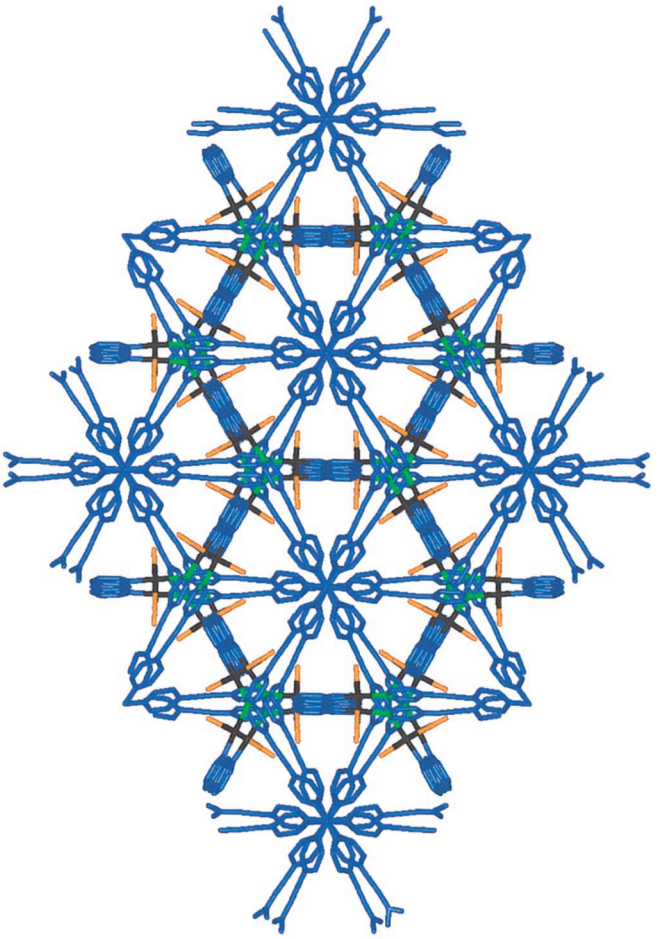

Fig. 3. Crystal packing diagram of **3c** as viewed down the {001} direction.

After the reactions were judged to be complete by NMR, each product was isolated as its hexafluorophosphate salt by precipitation with excess KPF_6.

Additional support for these structures was provided by ESI-MS. Analysis of the hexafluorophosphate salts of **3a–3c** all showed prominent $M - 2PF_6$ and $M - 3PF_6$ peaks (isotopically unresolved). Interestingly, the respective 2^+ and 3^+ peaks for **3a** at m/z 2,069 and 1,331 were found to be consistent with only five of the six nitrate counterions exchanged for PF_6^-. This formulation was also supported by elemental analysis. The nature of this distinction was revealed by single crystal x-ray analysis of **3a**.

Quality single crystals of **3a** grew after 2 days at ambient temperature by vapor diffusion of diethyl ether into a concentrated acetonitrile solution of the complex. It crystallizes in the triclinic system (space group $P\bar{1}$) with an asymmetric unit cell that contains a whole molecular prism, an NO_3^- and five PF_6^- anions. The entire molecular prism is situated so as to void any crystallographically imposed symmetry on the molecule. However, a pseudo-3-fold rotation axis can still be identified to run through the two OH groups. The most significant feature is that a nitrate anion was found incarcerated inside the cavity of the cationic complex (Fig. 1). It appears to be strongly bound because it was not exchanged, even in the presence of a large excess of KPF_6. It is interesting to note that the principal molecular axis of the NO_3^- is approximately in alignment with the pseudo-C_3 axis of the prism; the three oxygen atoms of the nitrate anion extrude into the space created between the molecular "clips." It is tempting to conjecture that the size and symmetry match between the supermolecular cation and the nitrate anion may contribute a great deal to this cation–anion affinity. As a point of note, the assembly of **3a** was observed to be about an order of magnitude faster than the formation of **3b** and **3c**. This finding suggests that the nitrate anion is possibly providing a templating effect, facilitating the formation of **3a**. Computer-generated van der Waals surfaces based on the x-ray data show that the NO_3^- fits securely inside the host framework. The solid-state asymmetry of the molecule is probably caused by an outward distortion of the Pt–N bonds that appear to be a result of slightly mismatched angles between the rigid molecular subunits; the average *trans*-(C—Pt—N) bond angle is about 174°. The dimensions of **3a** offer a more detailed description of the overall topology. The diameter is ≈19.1 Å, as defined by a circle that the arms of the propeller sweep out when rotated on its 3-fold axis (measured to the centroids of the anthracenes). The height, as defined by the distance between the central carbon atoms of ligand **3a**, is 9.34 Å. As expected, the pyridine groups were found perpendicular to the coordination planes of the platinum metal centers.

Single crystals of the BF_4^- salt of **3b** were grown from a DMF/Et_2O solvent system. Examination and geometric data collection of three single crystals from different batches of samples consistently revealed that **3b** crystallizes in the C-centered orthorhombic system with a = 54.868(4) Å, b = 76.086(4) Å, c = 27.958(2) Å, and V = 116714(1) Å3. Intensity data collection on a yellow-orange single crystal with dimensions of 0.33 × 0.25 × 0.21 mm at −100°C afforded a total of 483,454 reflections. The systemic absence of the reflections suggested the possible space group to be $C222_1$. Unfortunately, neither Patterson approaches nor direct methods have yielded any reasonable structure solution thus far. However, given that the NMR spectra and the ESI-MS data for **3b** are consistent with the smaller prism (**3a**, see above), as well as the larger prism (**3c**, see below), the structures of which have both been unambiguously determined by x-ray crystallography, the structure of **3b** can be assigned as a trigonal prism with a high degree of confidence.

Quality single crystals of the largest assembly in this series, metalla-prismatic cage **3c**, grew over the course of 1 week at ambient temperature by vapor diffusion of diethyl ether into a concentrated DMF solution of the complex. The asymmetric unit cell of **3c** (space group $R\bar{3}c$) contains half of a molecular "clip" (**1**) and a third of ligand **2c**. The entire molecular trigonal prism is generated by means of a 3-fold rotary inversion axis that runs through the central carbon atoms of the ligands (Fig. 2). Therefore, the molecule possesses crystallographically imposed D_{3h} symmetry. Because of the domination by the heavy Pt atoms on the electron density maps, three terminal carbon atoms on the triethylphosphine ligands could not be located from the difference Fourier maps. On the other hand, the PF_6^- ions are located completely outside the prism, and situated near a 2-fold rotation axis, making it crystallographically disordered. The structure refinement of **3c** was based on a model reflecting such disorders and gave $r = 0.149$. The packing diagram shows that the molecular prisms stack on top of each other along the crystallographic {001} direction (Fig. 3). Because the molecular axes of the prisms coincide with each other and the molecular clips from the neighboring prisms are in a staggered conformation, propeller-like hexagonal patterns are generated by the cations packed throughout the crystal lattice. The greater flexibility of the arms of the ligand could account for the higher symmetry in the solid-state structure of **3c** vs. **3a**. This bending is accommodated primarily by the acetylenic moieties. The overall dimensions of this structure are about 38 Å in diameter, with a distance of about 11.5 Å separating the central carbon atoms of ligand **2c**. These dimensions place **3c** among the largest discrete metallacyclic assemblies characterized by x-ray crystallography to date.

Conclusions

In summary, metalla-bicyclic supramolecular cages **3a**–**3c** were prepared by means of spontaneous self-assembly based on a molecular "clip" (**1**) as a rigid modular subunit. Multinuclear NMR and ESI mass spectral data, in conjunction with x-ray crystallography, unambiguously established their structure, which showed that the sizes of the propeller-type three-dimensional structures range from 1×2 nm to 1×4 nm. The formation of the smallest of these structures, **3a**, was accompanied by the entrapment of a nitrate ion inside its molecular cavity. Although the chemistry of metal-assembled molecular containers is steadily expanding, many of the desired features of that comprise guest selectivity are far from fully developed. Anionic guests appear to be the simplest and easiest starting points for controlled studies of inclusion phenomenon because of the inherent electrostatic affinity for the host framework. Ongoing investigations for this and related series of structures are being undertaken to assess the desired features of guest selectivity, reversibility, and dynamics.

We thank the National Science Foundation (Grant CHE-9818472) and the National Institute of Health (Grant 5R01GM57052) for support.

1. Holliday, B. J. & Mirkin, C. A. (2001) *Angew. Chem. Int. Ed.* **40,** 2022–2043.
2. Fujita, M., Umemoto, K., Yoshizawa, M., Fujita, N., Kusukawa, T. & Biradha, K. (2001) *Chem. Commun.* 509–518.
3. Uller, E., Demleitner, I., Bernt, I. & Saalfrank, R. W., eds. (2000) *Structure and Bonding* (Springer, Berlin).
4. Swiegers, G. F. & Malefetse, T. J. (2000) *Chem. Rev.* **100,** 3483–3537.
5. Leininger, S., Olenyuk, B. & Stang, P. J. (2000) *Chem. Rev.* **100,** 853–908.
6. Caulder, D. L., Brückner, C., Powers, R. E., König, S., Parac, T. N., Leary, J. A. & Raymond, K. N. (2001) *J. Am. Chem. Soc.* **123,** 8923–8938.
7. Caulder, D. L. & Raymond, K. N. (1999) *Acc. Chem. Res.* **32,** 975–982.
8. Caulder, D. L. & Raymond, K. N. (1999) *J. Chem. Soc. Dalton Trans.*, 1185–1200.
9. Baxter, P. N. W., Lehn, J.-M., Baum, G. & Fenske, D. (1999) *Chem. Eur. J.* **5,** 102–112.
10. Chambron, J.-C., Dietrich-Buchecker, C. & Sauvage, J.-P., eds. (1996) *Comprehensive Supramolecular Chemistry* (Pergamon, Oxford).
11. Campos-Fernández, C. S., Clérac, R., Koomen, J. M., Russell, D. H. & Dunbar, K. R. (2001) *J. Am. Chem. Soc.* **123,** 773–774.
12. Campos-Fernández, C. S., Clérac, R. & Dunbar, K. R. (1999) *Angew. Chem. Int. Ed. Engl.* **38,** 3477–3479.
13. Scherer, M., Caulder, D. L., Johnson, D. W. & Raymond, K. N. (1999) *Angew. Chem. Int. Ed. Engl.* **38,** 1588–1592.
14. Klausmeyer, K. K., Wilson, S. R. & Rauchfuss, T. B. (1999) *J. Am. Chem. Soc.* **121,** 2705–2711.
15. McMorran, D. A. & Steel, P. J. (1998) *Angew. Chem. Int. Ed. Engl.* **37,** 3295–3297.
16. Hasenknopf, B., Lehn, J.-M., Boumediene, N., Leize, E. & Van Dorsselaer, A. (1998) *Angew. Chem. Int. Ed. Engl.* **37,** 3265–3268.
17. Fleming, J. S., Mann, K. L. V., Carraz, C.-A., Psillakis, E., Jeffrey, J. C., McCleverty, J. A. & Ward, M. D. (1998) *Angew. Chem. Int. Ed. Engl.* **37,** 1279–1281.
18. Vilar, R., Mingos, D. M. P., White, A. J. P. & Williams, D. J. (1998) *Angew. Chem. Int. Ed. Engl.* **37,** 1258–1261.
19. Hasenknopf, B., Lehn, J.-M., Boumediene, N., Dupont-Gervais, A., Van Dorsselaer, A., Kniesel, B. & Fenske, D. (1997) *J. Am. Chem. Soc.* **119,** 10956–10962.
20. Mann, S., Huttner, G., Zsolnai, L. & Heinze, K. (1996) *Angew. Chem. Int. Ed. Engl.* **35,** 2808–2809.
21. Hasenknopf, B., Lehn, J.-M., Kniesel, B. O., Baum, G. & Fenske, D. (1996) *Angew. Chem. Int. Ed. Engl.* **35,** 1838–1840.
22. Beer, P. D. & Gale, P. A. (2001) *Angew. Chem. Int. Ed. Engl.* **40,** 486–516.
23. Schmidten, F. P. & Berger, M. (1997) *Chem. Rev.* **97,** 1609–1646.
24. Antonise, M. M. G. & Reinhoudt, D. N. (1998) *Chem. Commun.*, 443–448.
25. Keefe, M. H., Benkstein, K. D. & Hupp, J. T. (2000) *Coord. Chem. Rev.* **205,** 221–243.
26. Chang, S. H., Chung, K. B., Slone, R. V. & Hupp, J. T. (2001) *Synth. Metals* **117,** 215–217.
27. Keefe, M. H., Slone, R. V., Hupp, J. T., Czaplewski, K. F., Snurr, R. Q. & Stern, C. L. (2000) *Langmuir* **16,** 3964–3970.
28. Sun, S.-S. & Lees, A. J. (2000) *J. Am. Chem. Soc.* **122,** 8956–8967.
29. Kang, J. & Rebek, J., Jr. (1997) *Nature (London)* **385,** 50–52.
30. Fujita, M., Kwon, Y. J., Washizu, S. & Ogura, K. (1994) *J. Am. Chem. Soc.* **116,** 1151–1152.
31. Fujita, M., Nagao, S. & Ogura, K. (1995) *J. Am. Chem. Soc.* **117,** 1649–1650.
32. Hiraoka, S. & Fujita, M. (1999) *J. Am. Chem. Soc.* **121,** 10239–10240.
33. Hiraoka, S., Kubota, Y. & Fujita, M. (2000) *Chem. Commun.*, 1509–1510.
34. Ikeda, A., Udzu, H., Zhong, Z., Shinkai, S., Sakamoto, S. & Yamaguchi, K. (2001) *J. Am. Chem. Soc.* **123,** 3872–3877.
35. Ikeda, A., Yoshimura, M., Udzu, H., Fukuhara, C. & Shinkai, S. (1999) *J. Am. Chem. Soc.* **121,** 4296–4297.
36. Sun, W.-Y., Fan, J., Okamura, T., Xie, J., Yu, K.-B. & Ueyama, N. (2001) *Chem. Eur. J.* **7,** 2557–2562.
37. Liu, H.-K., Sun, W.-Y., Ma, D.-J., Yu, K.-B. & Tang, W.-X. (2000) *Chem. Commun.*, 591–592.
38. Su, C.-Y., Cai, Y.-P., Chen, C.-L., Zhang, H.-X. & Kang, B.-S. (2001) *J. Chem. Soc. Dalton Trans.*, 359–361.
39. Manimaran, B., Rajendran, T., Lu, Y.-L., Lee, G.-H., Peng, S.-M. & Lu, K.-L. (2001) *Eur. J. Inorg. Chem.*, 633–636.
40. Lindner, E., Hermann, C., Baum, G. & Fenske, D. (1999) *Eur. J. Inorg. Chem.*, 679–685.
41. Fujita, M., Oguro, D., Miyazawa, M., Oka, H., Yamaguchi, K. & Ogura, K. (1995) *Nature (London)* **378,** 469–471.
42. Fujita, M., Yu, S.-Y., Kusukawa, T., Funaki, H., Ogura, K. & Yamaguchi, K. (1998) *Angew. Chem. Int. Ed. Engl.* **37,** 2082–2085.
43. Sun, X., Johnson, D. W., Raymond, K. N. & Wong, E. H. (2001) *Inorg. Chem.* **40,** 4504–4506.
44. Sun, X., Johnson, D. W., Caulder, D. L., Raymond, K. N. & Wong, E. H. (2001) *J. Am. Chem. Soc.* **123,** 2752–2763.
45. Sun, X., Johnson, D. W., Caulder, D. L., Powers, R. E., Raymond, K. N. & Wong, E. H. (1999) *Angew. Chem. Int. Ed. Engl.* **38,** 1303–1307.
46. Manna, J., Kuehl, C. J., Whiteford, J. A. & Stang, P. J. (1997) *Organometallics* **16,** 1897–1905.
47. Olenyuk, B. O., Levin, M. D., Whiteford, J. A., Shield, J. E. & Stang, P. J. (1999) *J. Am. Chem. Soc.* **121,** 10434–10435.
48. Kuehl, C. J., Huang, S. D. & Stang, P. J. (2001) *J. Am. Chem. Soc.* **123,** 9634–9641.
49. Kuehl, C. J., Mayne, C. L., Arif, A. M. & Stang, P. J. (2000) *Org. Lett.* **2,** 3727–3729.
50. Gallasch, D. P., Tiekink, E. R. T. & Rendina, L. M. (2001) *Organometallics* **20,** 3373–3382.
51. Fuss, M., Siehl, H.-U., Olenyuk, B. & Stang, P. J. (1999) *Organometallics* **18,** 758–769.
52. Stang, P. J., Olenyuk, B. O. & Arif, A. M. (1995) *Organometallics* **14,** 5281–5289.
53. Brown, J. M., Pérez-Torrente, J. J. & Alcock, N. W. (1995) *Organometallics* **14,** 1195–1203.
54. Alcock, N. W., Brown, J. M. & Pérez-Torrente, J. J. (1992) *Tetrahedron Lett.* **33,** 389–392.